Binary Hairy Nanoparticles: Recent Progress in Theory and Simulations

Cangyi Chen, Ping Tang, Feng Qiu

Department of Macromolecular Science, State Key Laboratory of Molecular Engineering of Polymers, Fudan University, Shanghai 200433, China

Correspondence to: F. Qiu (E-mail: fengqiu@fudan.edu.cn)

Received 24 April 2014; revised 23 May 2014; accepted 27 May 2014; published online 16 June 2014

DOI: 10.1002/polb.23528

ABSTRACT: Binary polymer brushes, including mixed homopolymer brushes and diblock copolymer brushes, are an attractive class of environmentally responsive nanostructured materials. Owing to microphase separation of the two chemically distinct components in the brush, multifaceted nanomaterials with functionalized and patterned surfaces can be obtained. This review summarizes recent progress on the theory and simulations related to binary polymer brushes grafted to flat, spherical, and cylindrical substrates, with a focus on patterned morphologies of multifaceted hairy nanoparticles, an intriguing class of hybrid nanostructured particles (e.g., nanospheres and nanorods). In particular, powerful field theory and particle-based simulations suitable for revealing novel structures on these patterned surfaces, including self-consistent field theory and dissipative particle dynamics simulations, are emphasized. The unsolved yet critical issues in this research field, such as dynamic response of binary polymer brushes to environmental stimuli and the hierarchical self-assembly of binary hairy nanoparticles, are briefly discussed. © 2014 Wiley Periodicals, Inc. J. Polym. Sci., Part B: Polym. Phys. **2014**, *52*, 1583–1599

KEYWORDS: binary polymer brushes; curvature; hairy nanoparticles; microphase separation; nanoparticles; patterned surfaces; phase behavior; structure; surfaces; theory and simulations

INTRODUCTION Polymer brushes are composed of polymer chains tethered by end segments to a solid surface through either covalent bonding or physical adsorption.[1–4] From a historical perspective, polymer brushes initially found their applications in areas such as colloid stabilization,[2,5] wetting surfaces,[6,7] antifouling surfaces,[8,9] and improvement of lubrication properties.[10,11] In recent years, a rich variety of polymer brushes have been accurately synthesized with the boom of new polymerization techniques. Benefiting from this, polymer brushes have moved into a more diverse scientific realm.

In general, polymer brushes can be classified in different ways based on the chemical architectures of the grafted chains and geometry of the substrates, the simplest case is the linear homopolymer brushes grafted in planar substrates.[1–4] In addition, grafted star polymers,[12,13] comb polymers,[14,15] and dendritic polymers[16,17] have also been investigated. An important variation is the binary mixed polymer brushes, which refer to two immiscible homopolymers with their end segments grafting onto the same substrate by chemical bonding. Owing to the fixed grafting sites, microphase separation between the two chemically distinct linear chains can occur, resulting in interesting mesophase ordering in the soft grafting layers.[18–24] When mixed homopolymer brushes are replaced by end-grafted block copolymers, similar ordered mesophases are also possible to exist.[25–29] In addition to neutral polymer chains, another type of emerging polymer brushes is the charged polymer brushes in which the appearance of the long-range electrostatic interactions could lead to much more complex behaviors than that in neutral brushes.[30–34]

Although the most frequently studied systems are flat substrates,[6–9,35–37] in recent years, polymer brushes grafted onto nanoparticles with curved surfaces are also attracting more and more attentions.[3,38–48] The sizes of the core particles range from a few nanometers (e.g., gold nanoparticles and quantum dots) to hundreds of nanometers (e.g., silica or organic colloids). Polymers grafted at the inner surfaces of cylindrical pores [49–53] or spherical cavities[54,55] are also of interest.

To date, polymer brush has turned into an attractive issue related to chemistry, physics, biology, and engineering, and hence it is hard to enumerate all aspects of polymer brushes in a short review. Here, we restrict attention to binary polymer brushes on curved substrates, that is, the binary "hairy" nanoparticles (Scheme 1). For other special topics on polymer brushes, the reader is referred to recent reviews

© 2014 Wiley Periodicals, Inc.

Cangyi Chen received his B.E. degree in Polymer Materials Processing Engineering from Sichuan University, China, in 2011. He is currently pursuing a Ph.D. degree in Polymer Chemistry and Physics at Fudan University under the supervision of Feng Qiu. His main research interests are focused on the microphase behaviors of mixed polymer brushes grafted onto particles and their hierarchical structures through self-consistent field theory, and the excluded volume effects in polymer physics through classical density functional theory.

Ping Tang received her B.S. and Ph.D. degrees from Sichuan University in China. She worked at Imperial College with Julia Higgins as a visiting scholar. She is currently professor of macromolecular science at Fudan University. Her current research interests include theory and numerical modeling of the conformation and phase behavior of semiflexible polymers and complex polymers grafted or confined in curved substrates.

Feng Qiu received his B.S. degree in Chemistry from Fudan University, Shanghai, China, in 1992, the Master degree in Engineering from Shanghai Institute of Metallurgy, Chinese Academy of Sciences in 1995, and the Ph.D. degree in Polymer Chemistry and Physics from Fudan University in 1998. From 1998 to 2001, he was a postdoctoral research associate at the Department of Chemical and Petroleum Engineering at University of Pittsburgh. In 2001, he joined Fudan University as an Associate Professor at the Department of Macromolecular Science, and was promoted to Professor in 2003. His research activities primarily involve the equilibrium and dynamical properties of complex block copolymers, polymer solutions, and thin films. He received China National Funds for Distinguished Young Scientists in 2006.

published elsewhere.[56–61] In terms of binary polymer brushes, the phase separation between the two immiscible components in the brush endows them with fascinating potential applications, including smart microfluidic channels,[62] drug delivery,[63,64] smart responsive materials,[65–71] nanoscale lithography,[72,73] patterned surfaces,[35–37] and catalysts.[74,75] Specifically, binary polymer brushes covalently grafted onto solid substrates may offer an alternative for producing patterned surfaces which are more robust than block copolymers films coated by physical methods.[36,37] Such nanoscale patterning provides a powerful and inexpensive means for creating characteristic sizes below those can be achieved by conventional photolithography. In addition, the behavior of binary polymer brushes is sensitive to environmental variations (e.g., temperature, light, solvent, etc.).[65–71] Both experiments and theories have demonstrated that the surface properties of polymer brushes can be reversibly switched by changing solvent selectivity.[65,70] This property provides a way to form smart responsive materials. Further, binary polymer-grafted particles can be designed as multivalent nanoparticles, namely, nanoparticles with precisely controlled numbers and locations of functional sites.[38–40]

The past decade has seen a rapid growth in both the experimental and the theoretical researches of binary polymer brushes. Zhao and Zhu[57] have summarized the progress of binary mixed polymer brush-grafted particles mainly from an experimental viewpoint. More recently, Binder and Milchev[60] have presented an elaborated review based on the elementary theoretical concepts of polymer brushes with the main focus on the basic physical concepts of single-component brushes. Hence, in this review, we aim to summarize the theory and simulations related to binary polymer brushes, especially binary polymer brush-grafted nanoparticles, which have evoked intense interests in the past two decades. We hope to provide a basic guide to both theoretical and experimental researchers in this realm.

The outline of this review is as follows: first, we briefly comment on theoretical and simulation methods that are frequently used, taking binary polymer brushes on flat substrates as an example. Then we focus on the theory and simulations about binary polymer brush-grafted nanoparticles, other topics include binary "bottle-brush" polymers,[76–78] where two immiscible side chains are grafted to a stiff backbone, the interaction between two polymer brushes, as well as self-assemble of binary hairy nanoparticles. Finally, we summarize the topics and provide a perspective on the future theoretical and simulation development of binary hairy particles.

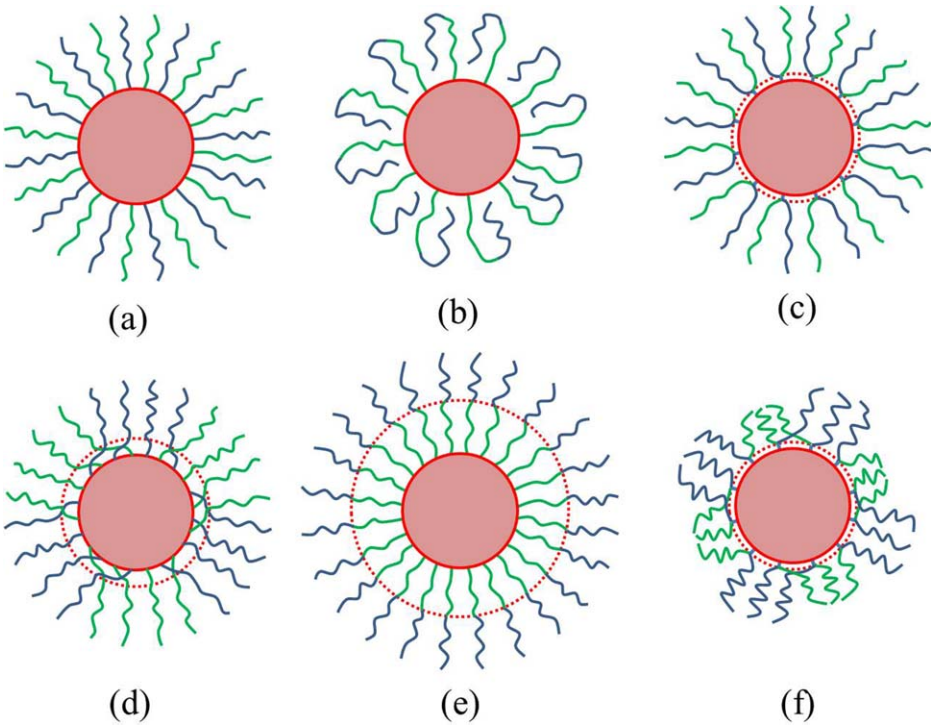

SCHEME 1 Spherical mixed homopolymer brushes in (a) homogeneous and (d) phase-separated states; spherical diblock copolymer brushes in (b) homogeneous and (e) phase-separated states; spherical Y-shaped diblock copolymer brushes in (c) homogeneous and (f) phase-separated states. A-component and B-component are shown by blue and green colors, and red region represents nanoparticle core. The dotted circle represents the interface between two layers.

BINARY POLYMER BRUSHES ON FLAT SUBSTRATES: METHODOLOGY AND CONCEPTS

The two simplest binary polymer brushes are as follows: mixed homopolymer brushes and diblock copolymer brushes. In the former, the end segments of the two immiscible homopolymer chains are randomly grafted onto a substrate (Scheme 1a), whereas the diblock copolymer brushes are composed of end-grafted diblock copolymers with sufficiently high grafting density (Scheme 1b). Particularly, there is a special diblock copolymer brush called Y-shaped brush in which the diblock copolymers are densely grafted on a substrate surface through a functional group at the junction point of the two blocks (Scheme 1c). The grafted Y-shaped copolymers can be viewed as a structural intermediate in between the grafted mixed homopolymers and the diblock copolymers. Both of these binary polymer brushes will undergo microphase separation which leads to domain structures on the nanometer scale. The phase behavior of binary polymer brushes on a flat substrate is controlled by a number of factors, such as monomer numbers of two chemically distinct species, incompatibility between the two components, grafting density, distribution of the grafting sites on the substrate, and environmental factors (e.g., solvent, polymer matrix, substrate, or surface properties). In this section, we will briefly comment on the theory and simulation methodology that involved in the research of mixed homopolymer brushes and diblock copolymer brushes on flat substrates, and take various examples from recent literature to illustrate the basic concepts of microphase separation in these brushes.

Methodology: A Very Brief Comment

Theoretical methods frequently involved in the research of binary polymer brushes include scaling arguments,[79–83] self-consistent mean field theory (SCFT),[35–40,84,85] single chain in mean field (SCMF),[70,86] and density functional theory (DFT).[9,67,87] Scaling theory is a powerful method in predicting the power law behavior that relates physical quantities (e.g., brush height and grafting density in a polymer brush). In the scaling arguments, one concentrates on crucial points from a simplified physical picture and usually ignores prefactors in the power laws. For instance, when polymers are grafted on a flat substrate at a sufficiently small grafting density σ, the individual chains do not interact with the adjacent chains, and they assume mushroom-like conformations. Consequently, the scaling laws of the brush height h in this regime is $h \approx 2R_g \propto N^{\nu}$ (R_g is the radius of gyration, N is the chain length, and ν is the Flory exponent). As the grafting density increases, the behavior of the grafted polymers transforms from mushroom-like to semi-dilute polymer brush.[88] In this case, according to the blob picture of Alexander,[81] the scaling of the brush height is $h \propto N\sigma^{1/3}$. At even higher graft densities (concentrated polymer brush), the scaling of the brush height becomes $h \propto N\sigma^{1/2}$. Based on

the scaling theory, the monomer density profile of polymers grafted on flat substrates is uniform for $z < h$ and zero for $z > h$ (z is the distance from grafting surface). When the polymers are grafted on a curved surface, the scaling laws of the polymer chains are different owing to the influence of the curvature. For the polymer chains grafted to a sphere of radius R, the total number of the grafting chains $n = 4\pi R^2\sigma$ is finite. According to the Daoud–Cotton picture,[89] the brush height obeys the law of $h \propto (n^{1/3}N)^{\nu} \propto (\sigma^{1/3}N)^{\nu}$.

SCFT is one of the most important field theoretic approaches to compute the properties of complex polymeric systems. It has been proven to especially suitable for investigating equilibrium morphology of polymer systems. Here, SCFT refers to a general method, whose essence is that the complex interactions in a many-chain system are replaced by one chain in an external field. The chain model can be Gaussian chain, wormlike chain, and other non-Markovian chains. Usually, SCFT means the classical SCFT, which is based on the ideal chains and the external field is replaced by a static mean field. Compared with scaling arguments, SCFT provides much greater details of the system structures, such as the segment probability and density distributions. On the other hand, the SCMF approach is also a mean field theory constructed from the free energy of a single chain in a self-consistent field. They differ in the way of how to calculate the chain conformational entropy. For example, in the SCMF developed by Müller,[86] the conformations of a single chain can be obtained by using Monte Carlo (MC) simulation. For this reason, SCMF is more suitable for dealing with nonideal chains, such as self-avoiding chains. In addition, in contrast to the SCFT, in which fluctuation effects are ignored, SCMF includes some fluctuation effects at the level of mean-field approximation.

Another type of mean field theory is the DFT, which is capable of capturing the effects that result from the size scale of individual monomers, such as strictly treatment of the excluded volume interaction, but this approach is somewhat difficult to treat two- or three-dimensional problems.

Different from the field-theoretical methods mentioned above, computer simulations take into account the interactions between the basic elements directly. In recent years, the simulation methods which are used in polymer brush systems include MC simulations,[90–93] molecular dynamics (MD) simulations,[60,94,95] coarse-grained particle simulations, such as Langevin dynamics,[96,97] Brownian dynamics (BD),[98] and dissipative particle dynamics (DPD).[99–101]

MC method, a statistical sampling method essentially, has been widely used in the research in polymer science. In this way, one can generate a stochastic trajectory through the phase space of the model considered and calculate the thermal averages of the physical quantities if one is interested in equilibrium states. The process of MC methods is composed of many basic technical pieces, such as random number generation, sampling methods, algorithms, lattice model, and off-lattice model, which can be found in dedicated reviews.[93,94]

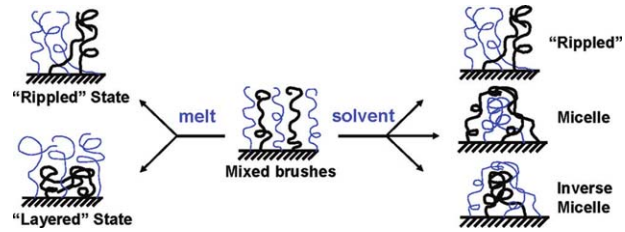

FIGURE 1 A simplified schematic illustration of self-assembly of mixed homopolymer brushes under equilibrium melt conditions and in various solvents. (Reproduced from ref. 57, with permission from American Chemical Society).

MD is a computer simulation of physical movements of atoms and molecules in the context of many-body simulation. In MD, the level of detail is dictated by the form of the force field, which can range from a fully atomistic to more coarse-grained potentials. In the atomistic MD simulations, the time steps employed in solving the equations of motion for the particles are on the scale of femtoseconds, and the computational time is prohibitive when one deals with polymer systems at large size or time scale. BD can be viewed as a simplified and coarse-grained MD, which is particularly useful when there is a large separation of time scales dominating the motion of different components of the system, such as polymers in a solvent. To access a large time step, the effects of solvent molecules on the polymers can be represented by dissipative and random force terms in solving the equations of motion of the system. Both BD and Langevin dynamics are based on the Langevin equation, whereas BD is a simplified Langevin dynamics, corresponding to overdamped systems in which inertia effects are negligible.

Another useful and powerful simulation method is the DPD, which allows the simulation of Newtonian and non-Newtonian fluids on mesoscopic length and time scales. Like MD and BD, DPD is a so-called particle-based method, but the elementary unit in DPD is just a point particle that represents a fluid element containing many molecules. In comparison to classical atomistic MD, although the coarse-grained BD or DPD loses the molecular level details, the reduction in computational time can extend these simulations to much larger systems. Hence, one should choose the appropriate methods based on the length and time scales of the specific problem.

Mixed Homopolymer Brushes: The Concept of Rippled and Layered Phases

Alexander[81] and de Gennes[82,83] were pioneers in investigating the properties of homopolymer brushes using scaling arguments in early 1980s, whereas the first theoretical work on mixed polymer brushes was carried out by Marko and Witten in 1991.[18] Under symmetric melt condition, they proposed the concept of a transition to a "rippled" phase—a density wave in composition running along the substrate surface (lateral microphase separation). This state is believed

to compete with a layered phase, rich in one component at the bottom of the brush layer, and rich in the other at the top (perpendicular microphase separation). The stability of these two phases was examined by assuming that the chains follow the "classical" path.[1] The results showed that the rippled phase tends to be the equilibrium structure, occurring at a molecular weight 2.27 times that for the same polymers in a simple blend at its demixing threshold. The ripple wavelength of the pattern was predicted to be 1.97 times the chain root-mean-square end-to-end distance. Later, the phase transition to the rippled phase in mixed brushes was further confirmed by applying the well-established random phase approximation.[102] Other researchers also studied the phase separation of mixed homopolymer brushes under melt condition.[19,103] Dong's[103] analytical work under mean field approximation indicated that a strongly phase-separated mixed brush must contain a phase-separated region and a mixed layer adjacent to the solid substrate. Brown et al.[19] performed large-scale MC simulations with the mixed homopolymers represented by self-avoiding walks on a simple cubic lattice. They observed lateral microphase separation after quenching the system from $\chi_{AB} = 0$ to $\chi_{AB} = 1$ when the chain length was fixed at $N = 100$, where χ_{AB} represents the Flory–Huggins parameter between the two species A and B.

The phase behavior of mixed polymer brushes has a strong dependence on the external environment (Fig. 1). Solvent can serve as an easily controllable external factor owing to the fact that its quality can be readily tuned from poor to good or selective. Lai[20] studied binary mixed brushes in a good solvent by bond-fluctuation MC simulations. In this case, symmetric mixed brushes also formed a rippled phase, but layered phase was observed by varying the relative fraction of the different components. Counter intuitively, the minority chains were more stretched and stayed away from the grafting surface. Subsequently, Soga et al.[104] provided more quantitative details about the microphase separation of mixed brushes in various solvent conditions by using a coarse-grained MC simulation that involves the direct calculation of the Edwards Hamiltonian. If the two species are sufficiently immiscible, lateral microphase separation is observed over a wide range of solvent conditions. Under poor solvent conditions, the combination of phase separation from solvent and phase separation of the two species themselves leads to interesting structural variations. Later, Müller[21] employed a general three-dimensional SCFT calculation to investigate the self-assembled structures of mixed brushes with quenched grafting points. He obtained the phase diagram of a mixed polymer brush as a function of stretching, composition, and incompatibility of polymer chains. At weak incompatibilities, different species aggregate into an array of parallel cylinders ("rippled" phase). At large incompatibilities or asymmetric compositions, two "dimple" phases were observed, where different species form clusters that arrange on a quadratic (checkerboard structure) or hexagonal lattice.

As the two homopolymer chains are chemically distinct, solvent selectivity plays an important role in determining the phase behavior. Upon exposure to a selective solvent, mixed brushes even with equal composition also exhibit a "dimple" structure in which the unfavorable component forms clusters. The experimental observations qualitatively agree with the SCFT study.[35] By using SCMF simulations, Wang and Müller[70] carefully constructed the diagrams of morphologies in various solvents as a function of grafting density and composition or chain-length asymmetry. Their comprehensive results almost covered all possible microphase structures of mixed polymer brushes in solvent.

When the mixed brushes are immersed in a selective solvent, even compatible or weak incompatible components will experience a phase separation. Xue et al.[99] employed DPD simulations to investigate the layered structure in mixed polymer brushes with compatible components in the cases of different chain lengths. The "phase-separation-like" behavior of compatible binary brushes, which is induced by the chain length difference, can be reversed by slightly changing the solvent selectivity. More recently, DFT was applied to study the perpendicular microphase separation of symmetric binary polymer brushes with weak incompatibility in selective solvents.[67] The results showed that the solvent selectivity is the necessary condition to trigger the perpendicular phase separation. Except for the static structures in thermal equilibrium, Merlitz and coworkers[89,97] also paid attention to the relaxation dynamics of phase transition of mixed brushes in selective solvent by using a Langevin dynamics approach.

Diblock Copolymer Brushes: Novel Structures Owing to Nontethered Free Blocks

The studies about end-grafted diblock copolymer brushes were carried out almost simultaneously with mixed homopolymer brushes. Theory and simulations on this important type of binary polymer brushes have been extensively reported in past two decades.[25,26,105–114] Similar to mixed homopolymer brushes, diblock copolymer brushes with enough incompatibility between the two blocks also experience microphase separation. In particular, in comparison to mixed homopolymer brushes, end-grafted copolymer chains own nontethered free blocks, and hence a variety of novel phase structures such as wormlike micelle, perforated layer, and "flower"-like structure have been predicated by varying relative block length, grafting density, interaction between different blocks and solvents.

The morphology of diblock copolymer brushes depends on the particular segment point at which the polymer is attached. First, we will discuss the properties of the Y-shaped copolymer brushes which are seen as a structural intermediate in between the mixed homopolymer and the end-grafted diblock copolymer brushes. In fact, owing to the tethered junction points, Y-shaped copolymer brushes are more similar to mixed homopolymer brushes. In 1996, Zhulina and Balazs[80] adopted scaling arguments to study the pattern formation of Y-shaped copolymer brushes in the melt and in the presence of a solvent. A rich variety of lateral nanostructures was predicted with different nonselective solvent quality, grafting density,

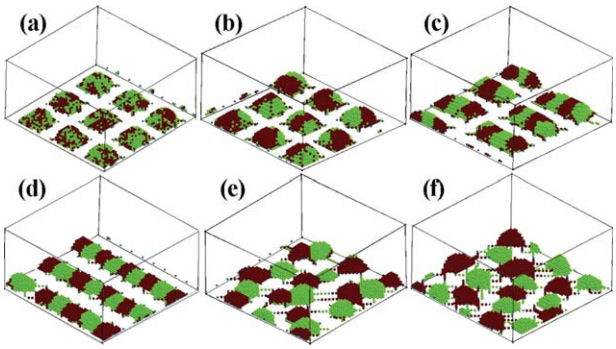

FIGURE 2 Typical morphologies of grafted Y-shaped copolymers in nonselective poor solvents at low grafting density. (a) Mixed micelles with $\varepsilon_{AB} = 0$; (b) internally segregated micelles with$\varepsilon_{AB} = 0.25$; (c) hamburger-like micelles with $\varepsilon_{AB} = 0.50$; (d) segmented wormlike micelles with $\varepsilon_{AB} = 0.75$; (e) connected micelles with $\varepsilon_{AB} = 1.2$; and (f) split micelles with $\varepsilon_{AB} = 3.0$. ε_{AB} is a reduced interaction energy between A-monomer and B-monomer. A-monomer and B-monomer are represented by different colors. (Reproduced from ref. 105, with permission from American Institute of Physics).

and incompatibility between the two blocks. In their studies, the densely grafted mixed brush is divided into two horizontal sublayers of thickness H_1 and $(H–H_1)$, where H is the fixed thickness of the brush and H_1 represents the thickness of the lower, mixed uniform layer. The width of the stripe phase in symmetric, highly incompatible systems is given by d. By minimizing the free energy of the system, the scaling law of the mixed uniform layer thickness related to the chain length N and incompatibility χ is $H_1 \propto N^{1/2}/\chi^{1/2}$ and the scaling law of the stripe width is $d \propto N^{1/2}$. In addition, the same scaling law in poor solvent becomes $H_1 = d \propto N^{1/2}(\tau^3/\chi)^{1/6}$ (τ is a parameter which indicates the solvent quality). Lately, the nanostructures of grafted Y-shaped copolymers were investigated via MC simulations using simulated annealing technique and DPD simulations.[105,106] Both of these simulations systematically examined how the solvent quality, the grafting density, and the incompatibility between the polymer blocks affect the morphology of the grafted layer. At low grafting density, interesting micellar structures can be observed, such as mixed micelles, internally segregated micelles, hamburger-like micelles, segmented wormlike micelles, connected micelles, and split micelles (Fig. 2).

Considering the melt state, Dong et al.[107] studied the phase behavior of end-grafted diblock copolymer brushes based on a mean field method. Subsequently, Brown et al.[108] employed MC simulations to the system of symmetric diblock copolymer brushes at near-melt condition. They found that the two monomer species vertically segregate to form a three-layer structure which is qualitatively different from lateral segregation of mixed homopolymer brushes. Zhulina et al.[110,112] expanded their studies to determine the phase behavior of end-grafted AB diblock copolymer brushes in selective solvent by using SCFT calculations and scaling arguments. Owing to the solvophobic interactions, "onion" or "garlic"-like micelles appeared while the solvent is poor for both components but the B block is assumed to be less soluble than the A block. On the other hand, if the solvent is poor for anchored B blocks, but good for the free A blocks, "flower"-like structure occurred, where the solvophobic Bs form the core of the "flowers," and the soluble As form the outer corona of "petals." These predicted phase structures were confirmed by more visualizable three-dimensional simulations.[27,28,112,113] More complicated structures formed by perpendicular segregation, lateral segregation, or their combination were observed (Fig. 3). Both of these theory and simulation results are in accordance with the available experiments.[115,116]

Long-Range Ordered Patterns: Key Role of Grafting Site Distribution

As mentioned above, both theory and simulations indicate that binary polymer brushes (either mixed or diblock brushes) on a flat substrate are an excellent candidate for forming patterned polymer films on nanometer length scales. This feature endows binary polymer brushes with potential to be used in next-generation information storage and electronic devices. Compared with block copolymer thin films, the tethering of chains will restrict the film to a monolayer preventing terrace formation. Furthermore, the grafted film should be more mechanically robust, which could allow it to be lightly sheared to remove the defects from the surface pattern.[25] However, the lack of long-range order and often defective microphases observed experimentally limits this

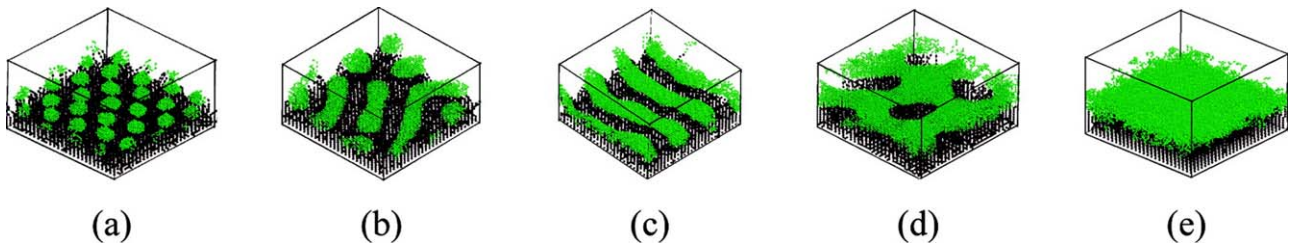

FIGURE 3 Morphologies of AB diblock copolymer brush for different length of the B-block with grafting density $\sigma = 0.25$ and length of A-block $N_A = 10$: (a) spherical micelles, $N_B = 4$; (b) wormlike micelles, $N_B = 8$; (c) stripe structure, $N_B = 10$; (d) perforated layer, $N_B = 16$; and (e) layer, $N_B = 20$. The A-monomers are shown as dark areas and B-monomers are light areas. (Reproduced from ref. 112, with permission from American Chemical Society).

application of such systems for lithography. Several possible reasons contribute to the loss of long-range order, such as the polydispersity of grafted polymer chains, ultra-slow microdomain dynamics in mixed brushes exceeding the entanglement threshold,[117] fluctuations of the grafting points, and so on. Among these factors, nonuniform grafting is considered to be the most predominant reason for the irregular domains observed experimentally.

Obviously, understanding the mechanism of losses of long-range ordered structures is urgent. It should be noted that all of the theoretical and numerical studies mentioned above have assumed that the grafting sites uniformly distribute on the surface. Nevertheless, spatial inhomogeneity of the distribution of grafting points is inevitable in experiments owing to the random nature of the grafting reaction. For diblock copolymer brushes, as all grafting points belong to the same species, the nonuniform grafting includes only the fluctuations in density. For mixed polymer brushes, however, both of the fluctuations in density and composition exit. By employing a MC simulation, Wenning et al.[92] demonstrated that for one-component brushes in a poor solvent and immiscible mixed homopolymer brushes, even weak density or composition fluctuations in grafting points can be amplified in the morphologies of the brush and prevent the long-range order in surface patterns. Both SCMF simulations and experiments were carried out by Santer et al.[118] to investigate the correlation between grafting points and morphology of conventional mixed brushes or Y-shaped brushes. The results showed that the statistical fluctuations of the chemical composition and domain memory[119] in the Y-shaped case are weaker than that in the mixed homopolymer brushes. Also using SCMF simulation, Wang and Müller[120] studied the memory effects of microphase segregation in diblock copolymer brushes and binary mixed homopolymer brushes exposed to the solvents of different qualities and selectivities. Memory effects are gauged by a fluctuation memory measure, which reflects the correlation between the fluctuations of grafting points and the microphase-separated morphology, and a domain memory measure, which quantifies the correlation between surface morphologies during cyclic exposure to different solvents. They pointed out that the two memory effects are closely correlated, and both of them have their root in the broken translational symmetry of the distribution of grafting points. Recently, Fredrickson group also concerned the details of strong correlation between the spatial distribution of the grafting points and the self-assembly of melt mixed brushes through SCFT.[37,121] They designed three different types of grafting density variations for each component by modulating the grafting chain end distribution functions while maintaining an uniform total grafting density. Their results demonstrated that microphase patterns are sensitive to both the wavelengths and the amplitudes of the imposed grafting density fluctuations. In addition, Fredrickson and coworkers[36] proved that long-range order in mixed homopolymer brushes on a flat substrate can be induced through a lateral confinement, but their directed self-assembly method was carried out under the assumption of uniform grafting distribution.

This section summarizes the theoretical and simulation studies related to mixed homopolymer brushes and diblock copolymer brushes on planar substrates. In the past two decades, many theoretical approaches have shown their unique advantages in exploring this region. To date, a quite deep understanding on the behavior of binary polymer brushes on flat substrates has been achieved. As a result of microphase separation between two immiscible components, a variety of surface nanostructures could be obtained by tuning chain (block) lengths, grafting densities, compositions, and incompatibility between the two components and solvents. As these surface patterns are sensitive to environmental variations, binary polymer brushes can be used as robust surface-responsive materials in technological applications. In addition, the self-assembled nanostructures of binary melt brushes have also attracted attention as a promising high-resolution lithographic tool if long-range order can be obtained. Theory and simulation results indicate that it is necessary to minimize the fluctuations in grafting points to achieve an improved long-range order. In comparison to mixed homopolymer brushes, Y-shaped or end-grafted copolymer brushes can decrease the fluctuations by suppressing composition fluctuation of grafting points. Another promising method is to arrange regular grafting points by crystallizing the end block of crystalline block copolymers.[122,123] Confinement or shear could also be exploited to improve the long-range order. All these developed methods and concepts derived in the planar substrate systems have proven to be the forward basis for the investigation of other type of substrates.

BINARY POLYMER BRUSHES ON CURVED SURFACES: "MULTIFACETED" HAIRY NANOPARTICLES

A new class of binary "hairy" particles can be obtained when polymers with two chemically distinct components are grafted onto the curved surface of particles with high enough grafting density. The binary "hairy" particles retain the nanopatterned and environmentally responsive properties as binary polymer brushes on the flat substrates. However, in comparison to binary brushes on flat substrates, these hybrid particles possess more complex and exciting properties owing to the existence of curved grafting surface. The previous theoretical studies have shown that the curvature of grafting surfaces has a great impact on the conformation of the grafted polymer chains.[3,90,124] For polymer chains on a convex surface, the chain will extend toward outside to gain more free space. The grafted chains on flat and curved substrates have different scaling laws that correlate the heights of brush and the lengths of chain.[88] Thus, the curvature undoubtedly plays an important role in determining the phase structures of binary brushes on particles. Another outstanding feature of these particles is interesting properties such as mechanical,[69,125] optical,[47,48] and magnetic properties,[126,127] which can be produced through choosing appropriate particle cores. The combination of two functionalized polymer components and core particles can lead to truly "multifaceted" hybrid nanoparticles that can incorporate multiple functionalities.[128–130] Furthermore, as basic building

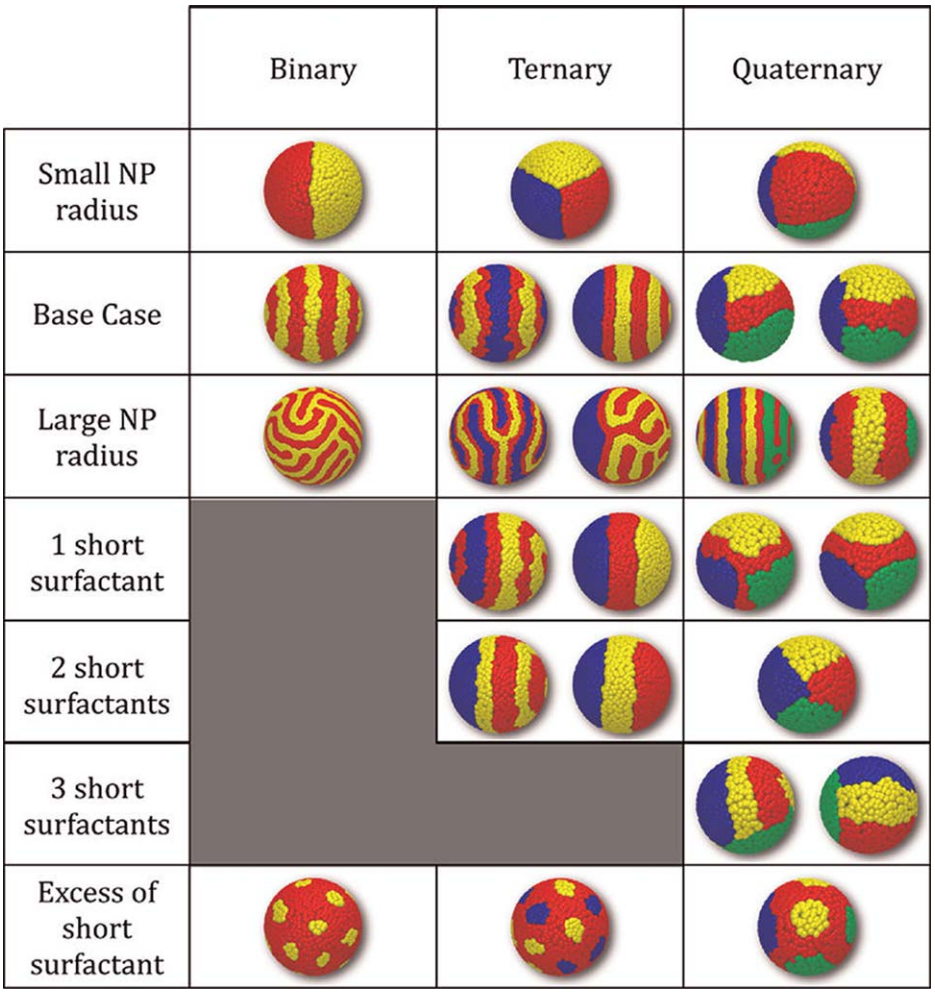

FIGURE 4 Patchy spherical nanoparticles made from binary, ternary, and quaternary SAMs adsorbed on gold nanoparticles (NPs). The head groups of the distinct ligands are shown in different colors (tails are not shown). The base case has a 1:1:1:1 stoichiometry, with symmetric length difference between ligands (3, 6, and 9 beads for ternary; 3, 6, 9, and12 beads for quaternary) on a NP of radius 4. (Reproduced from ref. 141, with permission from American Chemical Society).

blocks, "multifaceted" hybrid nanoparticles can assemble into hierarchically organized superstructures.[131,132]

"Multifaceted" Hairy Particles: Experimental Studies

Over the past decade, particles modified with two component polymer brushes have attracted enormous experimental interests. The core particles have been extended to a variety of nanomaterials including gold nanospheres[130–132] and nanorods,[46,133] silica nanospheres[41–45] and CdS nanoparticles.[134] Zhao and coworkers[41] synthesized mixed poly(tert-butyl acrylate)/polystyrene (PS) brushes with controlled molecular weights and narrow polydispersities from Y-initiator-functionalized silica particles. Subsequently, they systematically investigated how the phase-separation behavior was affected by parameters including solvent properties, polymer chain length and chain length disparity, overall grafting density, and curvature by using transmission electron microscopy (TEM).[42–45] In their silica-based hybrid particles, the diameter of silica core (~180 nm) is much larger than the size of the grafted polymers. Thus, the phase behavior of such large silica-based hybrid particles is closer to that of binary brushes on flat substrates. Another popular core particle is the gold nanoparticle (AuNP). Polymer chains with functional end groups such as thiols or disulfides can be easily tethered to the AuNP surface. However, although quite some two-component polymer brush-modified AuNPs have been studied for their stimuli-responsive properties and fascinating self-assembled superstructures, no reports that describe the nanopattern formation in two-component polymer brush coatings have appeared. Possible reasons are that the synthesis of well-defined high-density binary polymer brushes on such sized nanoparticles is difficult and characterization of the patterned structures in this scale is also challenging.

More experimental progresses in binary hairy particles can be seen in ref. 57. There Zhao and Zhu distinguished mixed brush-grafted particles by core radius: core radius significantly larger than the root-mean-square end-to-end distances $<R_{rms}>$ of the grafted polymers, core radius comparable to

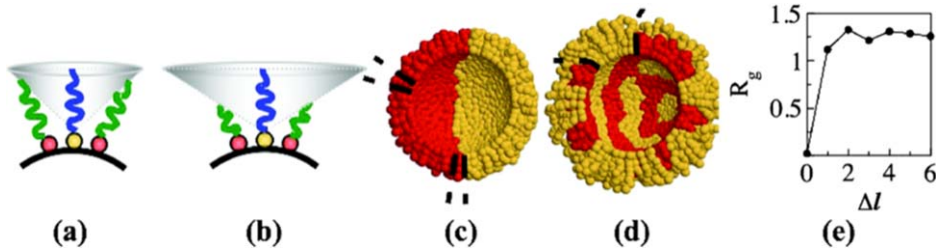

FIGURE 5 (a,b) Schematic two-dimensional representation of shared free volume (conical shaded area) available to ligand tails when they are surrounded by other equal-length and shorter ligands on curved surfaces, respectively. (c) Cross-sectional view of DPD simulation of equal-length ligands (length, 4) on a sphere of radius 5σ, showing that a ligand tail has the same available free volume (indicated by dashed lines). (d) Cross-sectional view of DPD simulation of unequal-length ligands (lengths, 4 and 8) on a sphere of radius 5σ, showing how the longer tails (yellow) fill the extra available free volume by bending over shorter ones (red) (shown by dashed lines). (e) Radius of gyration of long chains, R_g, versus length difference, Δl, with length of longer ligand fixed at 9. (Reproduced from ref. 139, with permission from American Physical Society).

$<R_{rms}>$, and smaller than $<R_{rms}>$. Essentially, this classification is based on the effect of substrate curvature on phase separation of the two chemically distinct components. As the polymer sizes are typically 10–50 nm, the first case can be represented by the silica-based hairy particles, whereas for core radius smaller than $<R_{rms}>$, one can find examples in the systems of polymer-grafted gold or silver nanoparticles. However, for the case of core radius comparable to the polymer size (in which the core size is in the range of tens of nanometers), there are rarely experimental examples except for the polymeric micelles with mixed chains in the corona layer.[135,136] Nevertheless, this "experimentally unchartered, intermediate territory" is attracting increasing attentions of the theoreticians.

Morphology of Binary Hairy Particles: Theoretical Models and Simulations

The phase behavior of binary polymer brushes grafted on flat substrates has been well investigated by theory and simulations as described previously. Transferring these concepts and methods from planar to curved surfaces of nanoparticles could open a way to "multifaceted" nanoparticles with patterned surfaces. The first theoretical work related to the nanopatterned hairy particles was performed by Roan in 2004.[38] Although over the last 10 years, a number of theoretical results have been published that describe the phase separation on the surface of nanoparticles, this area is still full of opportunities and challenges as compared to binary polymer brushes on flat substrates.

Binary Polymer Brushes on Nanospheres: Packing Frustration on Closed Surfaces

Before discussing the binary polymer-grafted nanoparticles, we will highlight some interesting results on a new class of materials: monolayer-protected metal nanoparticles with ordered domains in their ligand shell.[137,138] The self-assembled monolayers (SAMs) are composed of binary mixtures of immiscible thiolated molecules (or ligands). In a strict sense, the mixed thiolated molecules and binary polymer brushes are essentially different, but the two-component short molecules on small-metal nanoparticles can be seen as an analogous to binary polymers grafted onto particles with large radius. Using atomistic MD simulations and mesoscale DPD simulations, Glotzer and coworkers[139] investigated the formation of microphase-separated patterns on spherical nanoparticles covered by binary immiscible ligands. Their simulation results showed that Janus structure transfers into striped pattern, or "ripples" (Fig. 4, the second row) when the overall tail lengths, length mismatch, and the radius of nanospheres increase. In addition, they also studied the patterned structures of nanospheres covered by ternary and quaternary SAMs.[140,141] More novel surface patterns such as islands and multipatchy patterns can be found (Fig. 4). Taking the binary SAMs as an example, they revealed the origin of the observed patterns formed by immiscible ligands on the surfaces of gold or silver nanospheres. As the immiscible ligands are adsorbed on the surfaces (which makes them mobile), the Janus structure is considered to be a bulk phase-separated pattern. Although the formation of microphase-separated striped pattern creates additional interfacial energy compared to a bulk-separated system, but at the additional interfaces of the striped pattern the long ligand tails are adjacent to the shorter ones, which provides more free volume for the long ligands (Fig. 5). In other words, the striped pattern provides additional conformational entropy. If the entropy gain is sufficient, then microphase-separated stripes, rather than bulk phase separation, should occur as the equilibrium morphology. In other words, the microphase separation is a balance between the minimization of interfacial energy and the maximization of conformational entropy gain. The interesting surface patterns of these "short hairy" nanoparticles may provide some enlightening references when relatively short binary polymers meet large particles.

Early theoretical results of binary polymer brushes on nanoparticles were obtained by Roan using a fully three-dimensional SCFT calculation in spherical coordinate systems.[38,39] A variety of morphologies can be formed in the microphase separation of immiscible mixed homopolymer

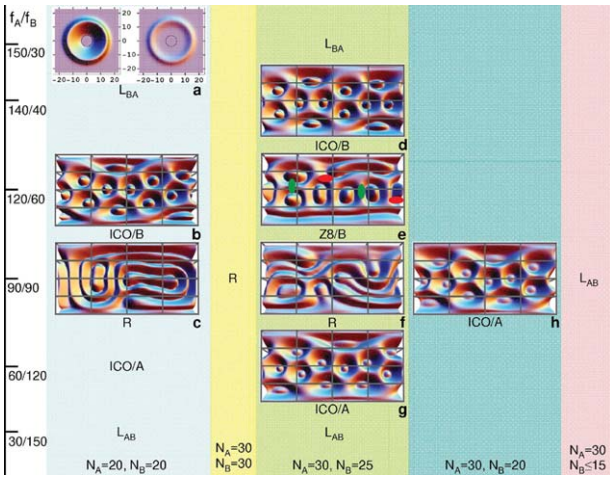

FIGURE 6 Structures at varying compositions but fixed total grafting density, $f_A + f_B = 180$, where f_A and f_B are the numbers of chains A and B, respectively. N_A and N_B are lengths of chains A and B. (a) Free-end distributions of A (left) and B (right); (b–h) World maps of total segment density, r (distance from the center of the particle) = 7. The radius of particles is 4, and Flory–Huggins interaction parameters between A and B, A and solvent, and B and solvent are 1, 0, and 0, respectively. (Reproduced from ref. 39, with permission from American Physical Society).

brushes on spherical nanoparticles with a radius comparable to the polymer size (Fig. 6). Like with the binary brushes on flat substrates, the phase structures can be tuned by compositions, polymer chain lengths, grafting densities, and distributions of the grafted ends. For instance, when the composition ratio f_A/f_B decreases from 150/30 to 90/90 with identical chain lengths, the equilibrium nanostructures change from layered L_{BA}, to 12-islanded ICO/B, and then rippled R [Fig. 6(a–c)]. The variation of chain length disparity with equal grafting densities also leads to a microphase transition. Furthermore, the rippled structures resulted from uniform grafting sites can be transformed into "giant-clam" structures by inhomogeneous grafting densities. In particular, the most interesting result is that "multivalent" nanoparticles with precisely controlled 3-, 6-, 8-, 9-, 10-, and 12-island structures can be formed in the microphase-separated spherical mixed brushes. Such structures of soft nanopolyhedras are similar to those found in small clusters of colloidal microspheres.[142] However, in Roan's study, "multivalent" nanoparticles with 2-, 4-, 5-, 7-, and 11-islands were missing. Wang et al.[40] also employed SCFT to investigate the microphase separation of mixed homopolymer brushes grafted onto a nanosphere in a nonselective solvent. In Cartesian coordinates, they embedded the sphere within a larger cubic computational cell and adopted a "masking" technique to treat the spherical boundary. The so-called masking technique originally proposed by Khanna et al.[143] introduces a cavity filed with hyperbolic tangent functional form to obtain the smooth boundary condition of a sphere. This numerical technique can circumvent the "pole problem" owing to the use of a spherical coordinate system in conventional finite difference or finite element grid. They also investigated the effect of the total grafting density, composition, and chain length asymmetry on the phase structures. Specially, they found that the sphere radius (i.e., substrate curvature) plays a significant role in determining the type of island structures, and a variety of islanded structures with the island numbers ranging from 2 to 8 are obtained by decreasing the curvature of the spherical substrate (Fig. 7).

For diblock copolymer brushes on spherical particles, Vorselaars et al.[144] have developed a new SCFT algorithm to solve the diffusion equations with a pseudo-spectral method that combines a spherical-harmonics expansion for the angular

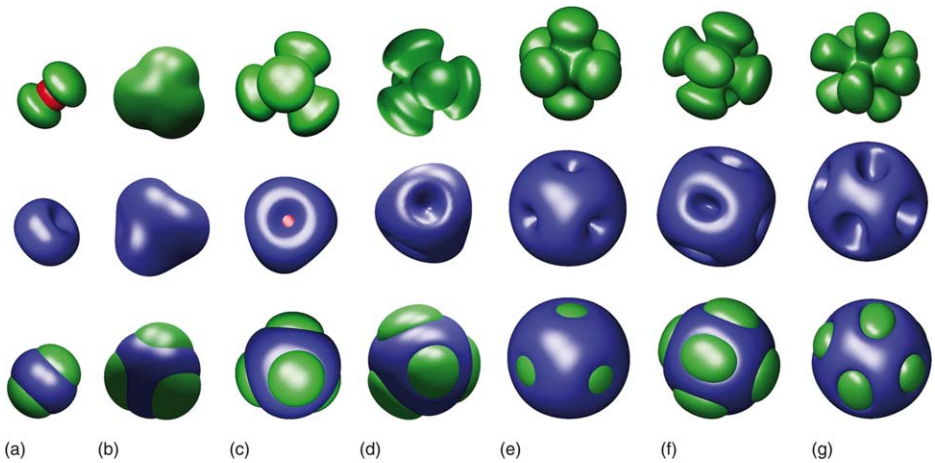

FIGURE 7 Typical structures with island number ranging from 2 to 8 at $\sigma_B/\sigma_A = 2.0$. From (a) to (g), the sphere radius increases from 0.5 to 4.0.The first and second rows are only A and B blocks, respectively, and the bottom row is isosurface morphologies of mixed polymer brush. The two polymer species A and B are represented by green and blue color, respectively, with a red sphere inside. (Reproduced from ref. 40, with permission from American Institute of Physics).

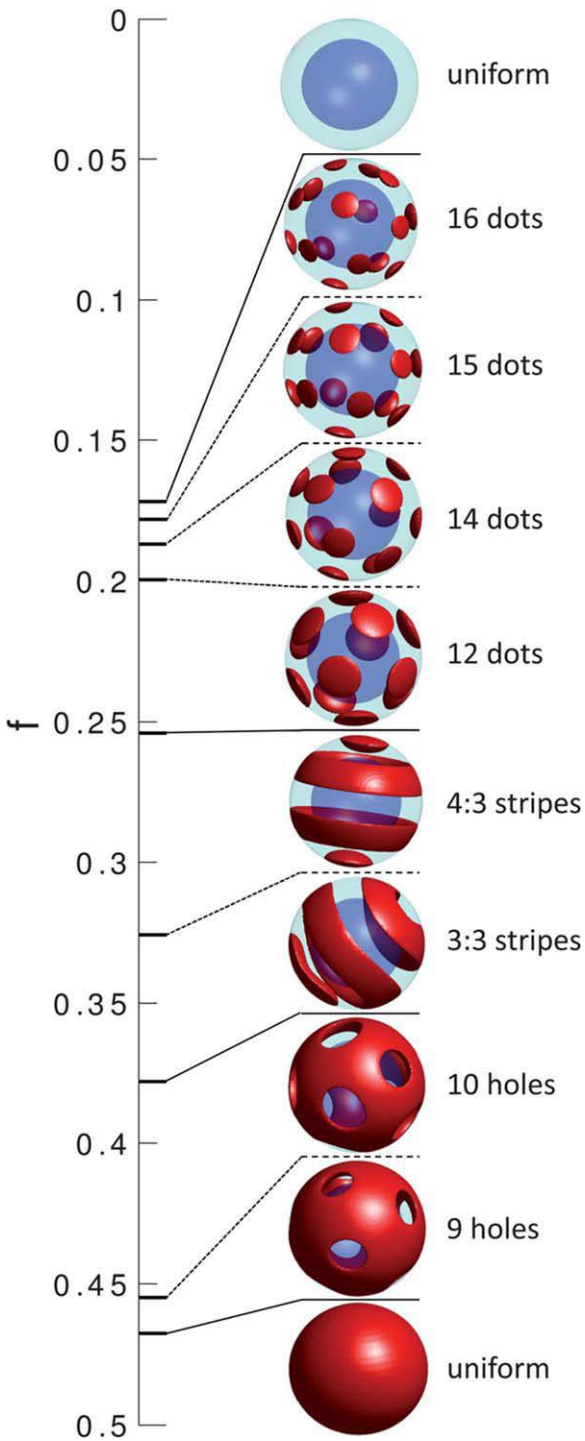

FIGURE 8 Stable morphologies for diblock copolymers grafted to the surface of a spherical core for $\chi N = 25$, $L = 0.5R_0$, and $R_c = R_0$. Here χN, L, R_0, and R_c represent Flory–Huggins interaction parameters between A and B, thickness of film, end-to-end length of copolymers, and core radius, respectively. The A-rich domains are shown in red and the B-rich domains are omitted. (Reproduced from ref. 144, with permission from Royal Society of Chemistry).

coordinates with a modified real-space Crank–Nicolson method for the radial direction. Using this algorithm, the sequence of the equilibrium patterned structures was predicted as a function of the diblock copolymer composition. As the volume fraction of the nontethered free blocks increases, the domains of the free blocks transform from dots to stripes to a layer with holes and finally to a uniform shell (Fig. 8). Furthermore, they also discussed the details on how the phase behavior is affected by the constraint of a finite surface area from a viewpoint of packing frustration. The distribution of dots (or holes) on the spherical surface, which is influenced by frustration effect resulting from the finite surface area, is similar to Thomson problem.[145] Then, by implementing the unit-cell approximation routinely used in the study of bulk systems, the computational cost of the calculation was greatly reduced.[29] The reduction in computational time provides a possible way to map out the phase behavior more extensively and consider much larger particles.

As described above, we know that the microphase behavior of binary polymer brushes on spherical nanoparticles with a radius comparable to the polymer size exhibits some similarities to the binary brushes on flat substrates, but the curvature and the constraint of a finite surface area contribute a unique property. Particularly, these results suggest a route to fabricate "multivalent" nanoparticles, namely, nanoparticles with precisely controlled numbers and locations of functional sites. On the other hand, we note that there are rare reports regarding phase behavior of binary polymer brushes on the nanosphere with a radius smaller than the size of the grafted polymers. Only Dong and Zhou performed a coarse-grained simulation to study the solvent responsive of AuNPs modified with amphiphilic polymer brushes.[146] Both PS–PEO block copolymers and binary-mixed PS/PEO brushes were considered. In five different solvents, typical core–shell, Janus-type, buckle-like, ring-like, jellyfish-like, and octopus-like morphologies were obtained (Fig. 9). When the radius of the spherical core is much smaller than the polymer size, the limiting case is AB_n miktoarm star copolymer, whose phase structures have been investigated extensively.[147,148]

Binary Polymer Brushes on Nanorods: Influence of Anisotropic Curvatures

Ordered patterns on nanorods are of particular interest for potential applications in the fields of molecular recognition, microelectronics, and catalysis.[74,149,150] Owing to an elongated geometry, the phase behavior of binary polymer brushes on nanorod will be more complex. For both planar and spherical substrates, the curvature at each position on the surface is constant, either zero or uniform. Therefore, preference of different orientations in microphase structure is lost. However, when considering a cylindrical nanorod, the chain extensions in the radial, axial, and lateral directions are different owing to the inhomogeneous curvatures in different directions along the substrate.

The model of mixed SAMs on spherical nanoparticles can be extended to the nanorod situation straightforwardly. DPD

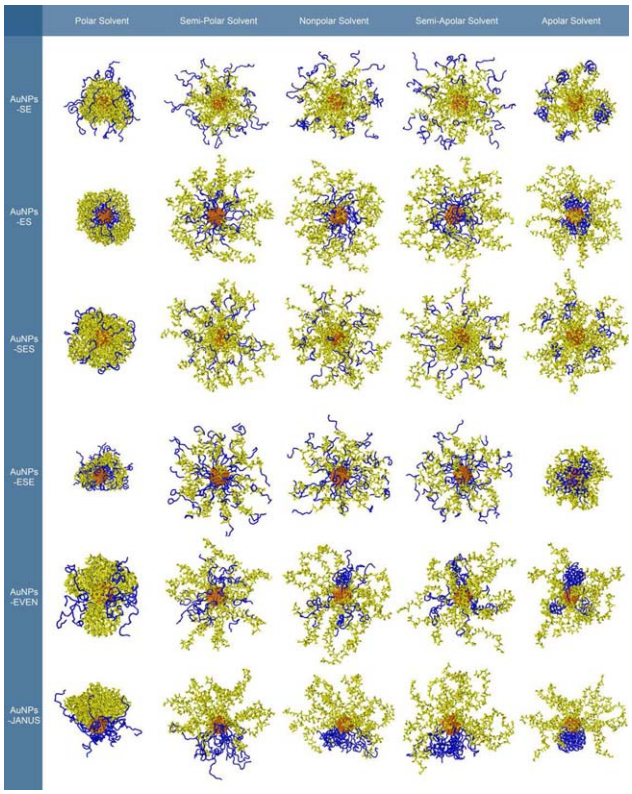

FIGURE 9 Equilibrium morphologies of six two-component polymer brush-modified AuNP systems in five solvents (polar, semi-polar, nonpolar, semi-apolar, and apolar) .Typical core–shell, Janus-type, buckle-like, ring-like, jellyfish-like, and octopus-like morphologies are formed. (Reproduced from ref. 146, with permission from WILEY-VCH Verlag GmbH & Co. KGaA, Weinheim).

simulations have been carried out to investigate nanoscale-striped patterns in the incompatible mixed SAMs on nanorods or nanowires.[151] The two-component ligand molecules on nanowires can also be viewed as a limiting case in which relatively short polymers are grafted onto cylinders of large radius. The simulation results showed that the two length-mismatched and incompatible ligands self-organize into equilibrium alternating stripes which are always perpendicular to the nanowire axis [Fig. 10(a)]. The stability of the perpendicular stripes (which are rings) against the parallel stripes is discussed by considering the potentially conformational entropy gain of the long ligands arranged in the perpendicular stripes relative to the parallel stripes. As shown in Figure 10, in the perpendicular stripes, the long ligands gain more free volumes not only along the circumference of the cylinder owing to the surface curvature, but also along the axis owing to the bending of the long ligands over the adjacent short surfactants. However, crowding of the long ligands occurs along the axis in the parallel stripes. Therefore, rings perpendicular to the cylinder axis are always entropically favored over parallel stripes. They also pointed out that the width of the stripe can be tuned by varying degrees of incompatibility, different length mismatches, and curvature of the cylindrical substrate.

Inspired by the stripe-like patterns in the systems of mixed SAMs adsorbed on a cylindrical substrate, Miller et al.[152] and Egorov[153] studied the phase separation of mixed polymer brushes anchored on cylindrical surfaces by using DPD simulation and SCFT, respectively. The ring-shaped alternating stripes perpendicular to the cylinder axis were observed in both studies. Furthermore, phase separation of mixed polymer brushes with different chain lengths on surfaces with nonuniform curvature was investigated by combining the MD simulation and a simple scaling theory.[154] Based on these studies, a general observation is that, on a surface with nonuniform curvature, the longer chains tend to locate in high curvature regions, and the numbers of striped domains are typically limited by the nonuniform curvature.

However, in the aforementioned cases mobile grafting sites are permitted and the nanorods own large or infinite aspect ratio (i.e., the nanorod length is much larger than its radius). Recently, Ma et al.[155] employed three-dimensional SCFT to investigate the microphase structures of binary mixed polymer brushes grafted on nanorod particles in a nonselective solvent. Phase diagrams involving a series of system parameters, such as the aspect ratio of the nanorod, the grafting density, and the chain length were constructed (Fig. 11).

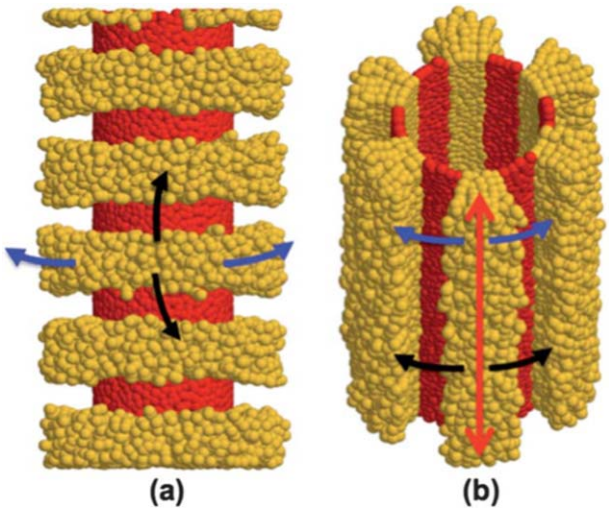

FIGURE 10 Directions in which the free volume and conformational entropy can be gained by the long (yellow) ligands when stripes are formed (a) perpendicular to, and (b) parallel to the cylindrical axis. Tails of the short (red) ligands have been removed for clarity. Blue arrows indicate the direction in which the long ligands gain free volume owing to the curvature of the substrate. Black arrows indicate the direction in which the long ligands gain free volume by bending over the neighboring short ligands. Red arrows indicate the direction in which crowding of the long ligands occurs. (Reproduced from ref. 151, with permission from Royal Society of Chemistry).

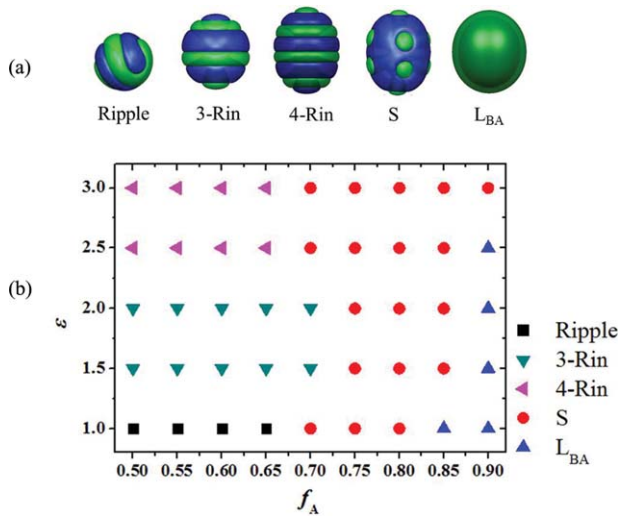

FIGURE 11 (a) Morphologies of typical structures of the brush-rod system ($\chi_{AB}N = 40$) with $N_A = N_B = 24$; (b) The phase diagram of the asymmetric brush-rod in terms of ε and $f_A = \sigma_A/(\sigma_A + \sigma_B)$. Here, the aspect ratio of the nanorod is denoted as $\varepsilon = (H + 2R)/2R$. (Reproduced from ref. 155, with permission from American Institute of Physics).

Here, the nanorod is composed of a cylindrical body and two semi-spherical caps, and hence the geometric appearance is determined by radius and length–diameter ratio. Owing to the spatial constraint of the two semi-spherical caps and fixed grafting points, both the parallel ripple and perpendicular ring phases could occur. In addition, the difference of the free energy between the two phases has a strong dependence on solvent entropy, and hence they predicted that both the parallel ripple and ring phases are possible to be observed in experiments. Subsequently, they also investigated the microphase separation of mixed brushes on an infinitely long cylinder.[156] Without the spatial constraint of the two semi-spherical caps, regular parallel ripple phase and ring phase can be obtained more easily. According to the degree of phase segregation, they demonstrated that the ring phase tends to be the more stable morphology with the increasing of rod radius, grafting density, and incompatibility between the two distinct components.

In this part, we briefly introduce the theory and simulation results on phase behaviors of binary polymer brushes on cylindrical substrates. The asymmetry of curvatures along the circumference and axis of the cylinder leads to interesting patterns such as ring-shaped alternating stripes perpendicular to the cylinder axis. If the alternating rings are hydrophobic and hydrophilic, respectively, an interesting "multifaceted" nano-object that could find technological applications (e.g., site-isolated catalysts[74,75]) can be obtained. More important fact is that patterning on a cylindrical surface provides a better way to understand how curvature influences the phase separation of binary polymer brushes. On the other hand, when the geometric dimension of cylindrical substrates is much smaller than the polymer size, binary bottle-brush polymer occurs as a limiting case[76–78] in which binary side chains are grafted to either stiff backbone chains or flexible backbones at high grafting density. Microphase structures such as "pearl-necklace" type and "Janus dumbbell" type can be formed by varying the grafting density and the solvent quality.

Interaction between Binary Polymer Brushes: Toward Superstructures

Notably, the binary brush-grafted particles do not always appear as an isolated particle in experimental systems.[41–45] Therefore, it is important to understand the interactions between adjacent binary brush-grafted particles. Furthermore, the self-assembly of binary brush-grafted particles into superstructures is of great significance in creating novel functional nanomaterials.

The repel force when two homopolymer brushes come into close contact in good solvent is considered as a basic mechanism for colloid stabilization.[2,5] To date, the interaction forces and the properties of contacted homopolymer brushes (e.g., density distribution and brush height) have been widely studied. The details on this issue can be seen in ref. 60 in which the authors summarized the interactions between two planar homopolymer brushes, two spherical homopolymer brushes, as well as the interaction of polymer brushes with nanoparticles. In terms of two contacted binary polymer brushes, intuitively, the individual phase behavior of the two binary brushes may be affected by each other and the confined space between them. There is a possibility that attractive forces occur even in good solvent owing to the phase separation between the two incompatible components. Unfortunately, only very few elaborate theoretical or experimental studies have been performed regarding this problem. Using a two-dimensional SCFT, Singh et al.[157,158] investigated the interaction between two planar surfaces where each surface is alternately grafted with both A and B homopolymers in selective solvent. They found that the interaction-free energy has a large attractive region at low grafting densities even if one of the components is in a good solvent. The attraction between the surfaces is owing to the formation of novel self-assembled structures when the surfaces are in contact with each other. So far, no report has been published that describes how the interaction between two binary hairy particles affects the phase separation.

When multiple binary brush-grafted particles meet each other, another more interesting topic comes forth, that is the hierarchical self-assembly of the binary brush-grafted particles. As it is well known, a variety of substances have been used to decorate the surface of nanoparticles, such as charges,[159,160] tethered oligomers,[161] mixed SAMs,[162] grafted dendrimers,[163] homopolymer brushes,[164,165] and DNA linkers, [166,167] which has led to far richer packing structures than that of pure nanoparticles. There are also some experimental studies on the superstructures of binary brush-grafted nanoparticles.[131,132] For example, Zubarev et al.[131] reported that one-dimensional cylindrical nanoarrays of

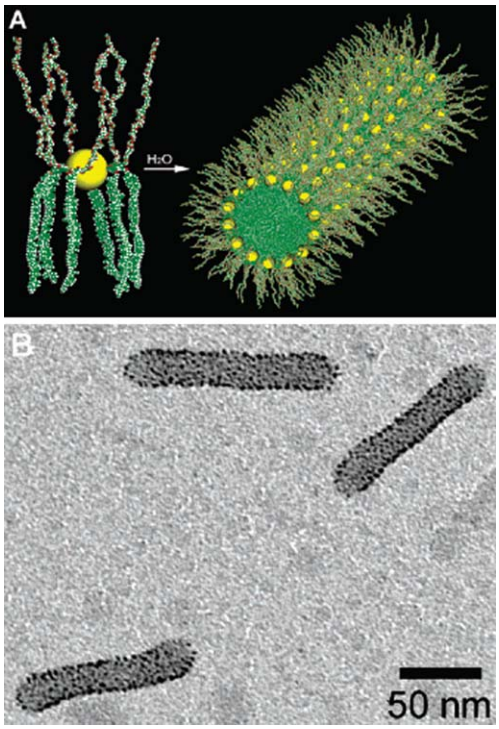

FIGURE 12 (a) Schematic representation of the self-assembly of Au nanopaticles grafted with amphiphilic Y-shaped PS-*b*-PEO block copolymers (for simplicity reasons only six PS-PEO molecules are shown). (b) TEM image of tubular assemblies of amphiphilic PS/PEO brush-grafted Au nanoparticles after dialysis of a THF/H_2O (1:3 v/v) solution against deionized water. (Reproduced from ref. 131, with permission from American Chemical Society).

AuNPs can be formed through self-assembly of AuNPs grafted by amphiphilic Y-shaped block copolymers. The well-defined cylindrical AuNP nanoarrays with a diameter of 18 nm and a length of 100 nm were observed by TEM (Fig. 12). Owing to the growing interest in the self-assembly of binary brush-grafted nanoparticles, theory and simulations, which can provide more physical insights and structure details about the self-assembly, are urgent. However, the huge computational load that is needed in exploring all the equilibrium superstructures of polymer-grafted particles is usually unaffordable. Jayaraman and coworkers[168,169] reported the assembly of copolymer-functionalized nanoparticles by using MC and coarse-grained MD simulations. In their dilute simulation systems, only 10–20 grafted nanoparticles are immersed in a large box consisted of solvents, and each nanoparticle contains only six grafted chains. The structures of the assembled nanoclusters have a strong dependence on the copolymer composition, monomer sequence, monomer–monomer interaction strengths, and particle sizes. Recently, Ginzburg[170] investigated the morphology of homopolymer-grafted nanoparticles in polymer melts by combining the SCFT for polymers with DFT for particles. This method has potential for the study of the superstructures assembled by binary brush-grafted nanoparticles.

CONCLUDING REMARKS AND OUTLOOK

Binary polymer brushes (i.e., mixed homopolymer brushes and diblock copolymer brushes) have attracted broad attentions owing to their novel nanoscale microphase structures and environmental responsive properties. In this review, we summarize recent advances in theory and simulations related to binary polymer brushes grafted on flat substrates and nanoparticle surfaces. In terms of planar binary polymer brushes, theory and simulation studies have been carried out for over two decades, and great progress has been made in understanding of their phase behaviors.

However, there are still some open questions that deserve to study, especially for binary hairy nanoparticles. Here, we list some unsolved issues from a theoretical viewpoint: (i) Most of the theoretical research has been focusing on the equilibrium patterned structures of binary hairy particles under the melt condition or in nonselective solvents. Even for binary polymer brushes on flat substrates, the effects of selective solvents on the patterned structures have been researched only in equilibrium states. However, the dynamic stimuli-responsive behaviors of binary polymer brushes are more interesting and valuable.[128,171,172] For example, when symmetric binary hydrophilic/hydrophobic polymer brushes are immerged in a hydrophilic solvent, the hydrophilic components will spread toward the outer layer. If the solvent quality changes from hydrophilic to hydrophobic, both chain layers have to move through each other in opposite directions. Unfortunately, the relaxation behaviors of the grafted chains in this process are unclear. Therefore, it is urgent to carry out theory and simulations to investigate how the different brush structures and properties are in response to environmental variations. (ii) To date, exciting progress on morphology of binary polymer brushes grafted onto curved surfaces has been made (e.g., nanosphere and nanorod). Although some preliminary understanding has been achieved on the substrate curvature effects, the morphology on a concave surface, for example, on the inner surface of a nanopore is still unknown. In contrast to the polymer brushes grafted on nanosphere or nanorod, the chains grafted on a concave surface will become more crowded when they spread out from the grafting surface. If the radius of the nanopore is comparable to the polymer size, then the interplay of the polymer phase separation and the closed substrate surface may play important roles in determining the self-assembled nanostructures in the brush. In addition, in selective solvents, a tube whose inner surface is coated by mixed homopolymer brushes can be used as a "smart channel."[62] (iii) In addition, the order–disorder transition (ODT) of binary polymer brushes deserves more considerations. First, although Marko and Witten predicted that the critical molecular weight for symmetric mixed brushes on a flat substrate to phase separate is 2.27 times that for the same polymers in a simple blend,[18] the effect of surface curvature on the ODT remains unexplored. It is interesting to know whether the ODT on curved surfaces will be different from that on the flat substrate and how it depends on the shape of the nanoparticles. Another more open question about the ODT of binary polymer

brushes can be raised while comparing with the microphase separation of diblock copolymers. When the incompatibility between the two blocks starts to trigger phase separation, the polymer chains are only weakly stretched. However, this circumstance is not suitable for binary polymer brushes at high grafting density; in this condition, the densely-grafted chains have already been strongly stretched owing to the excluded volume effects even when the two components remain in a mixed state. Therefore, phase separation should occur in highly elongated chains. To our knowledge, the influences of the stretched chain conformations on phase separation in binary polymer brushes have received much less attention.

Last but not least, binary hairy particles are often assumed to be isolated particles for convenience in theory and simulations. However, it is also important to understand the interactions between adjacent binary brush-grafted particles. Such interactions may in turn influence the phase behaviors of the neighboring binary brushes. Furthermore, the self-assembly of binary hairy particles into superstructures is of great significance. Like the charges, oligomerics, mixed ligand SAMs, dendrimers or DNA, binary polymer brushes can be used to functionalize the nanoparticles. Thus these hybrid "soft" particles, whose appearances can be deformed under different conditions, not only offer novel properties by assembling into various superstructures, but also offer unique opportunities for advancing the fundamentals of polymer physics. We have the reason to believe that a better understanding of the hierarchical self-assembly of binary hairy particles will be achieved in the foreseeable future.

ACKNOWLEDGMENTS

The authors are grateful to Lei Zhu and Bin Zhao for their communications on the experimental issues in polymer brushes. The authors also gratefully acknowledge the financial support from the National Basic Research Program of China (Grant No. 2011CB605700) and the National Natural Science Foundation of China (Grant No. 21320102005).

REFERENCES AND NOTES

1 S. T. Milner, T. A. Witten, M. E. Cates, *Macromolecules* **1988**, *21*, 2610–2619.

2 S. T. Milner, *Science* **1991**, *251*, 905–914.

3 C. M. Wijmans, E. B. Zhulina, *Macromolecules* **1993**, *26*, 7214–7224.

4 B. Zhao, W. J. Brittain, *Prog. Polym. Sci.* **2000**, *25*, 677–710.

5 D. H. Napper, Polymeric Stabilization of Colloidal Dispersions, Academic Press: London, **1983**.

6 A. Sidorenko, S. Minko, K. Schenk-Meuser, H. Duschner, M. Stamm, *Langmuir* **1999**, *15*, 8349–8355.

7 A. Johner, C. M. Marques, *Phys. Rev. Lett.* **1992**, *69*, 1827–1830.

8 K. Vacheethasanee, R. E. Marchant, *J. Biomed. Mater. Res.* **2000**, *50*, 302–312.

9 X. F. Xu, D. P. Cao, *J. Chem. Phys.* **2009**, *130*, 164901.

10 J. F. Joanny, *Langmuir* **1992**, *8*, 989–995.

11 J. Klein, Y. Kamiyama, H. Yoshizawa, J. N. Israelachvili, G. H. Fredrickson, P. Pincus, L. J. Fetters, *Macromolecules* **1993**, *26*, 5552–5560.

12 D. J. Irvine, A. M. Mayes, L. GriffithCima, *Macromolecules* **1996**, *29*, 6037–6043.

13 S. S. Sheiko, S. Panyukov, M. Rubinstein, *Macromolecules* **2011**, *44*, 4520–4529.

14 E. B. Zhulina, T. A. Vilgis, *Macromolecules* **1995**, *28*, 1008–1015.

15 H. Y. Zhao, X. L. Kang, L. Liu, *Macromolecules* **2005**, *38*, 10619–10622.

16 L. N. Gergidis, A. Kalogirou, A. Charalambopoulos, C. Vlahos, *J. Chem. Phys.* **2013**, *139*, 044913.

17 O. V. Rud, A. A. Polotsky, T. Gillich, O. V. Borisov, F. Leermakers, M. Textor, T. M. Birshtein, *Macromolecules* **2013**, *46*, 4651–4662.

18 J. F. Marko, T. A. Witten, *Phys. Rev. Lett.* **1991**, *66*, 1541–1544.

19 G. Brown, A. Chakrabarti, J. F. Mark, *Europhys. Lett.* **1994**, *25*, 239–244.

20 P. Y. Lai, *J. Chem. Phys.* **1994**, *100*, 3351–3357.

21 M. Müller, *Phys. Rev. E* **2002**, *65*, 030802.

22 B. Zhao, T. He, *Macromolecules* **2003**, *36*, 8599–8602.

23 B. Zhao, *Langmuir* **2004**, *20*, 11748–11755.

24 B. Zhao, R. T. Haasch, S. MacLaren, *J. Am. Chem. Soc.* **2004**, *126*, 6124–6134.

25 M. W. Matsen, G. H. Griffiths, *Eur. Phys. J. E* **2009**, *29*, 219–227.

26 D. Meng, Q. Wang, *J. Chem. Phys.* **2009**, *130*, 134904.

27 J. Wang, M. Müller, *Macromolecules* **2009**, *42*, 2251–2264.

28 O. A. Guskova, C. Seidel, *Macromolecules* **2011**, *44*, 671–682.

29 G. H. Griffiths, B. Vorselaars, M. W. Matsen, *Macromolecules* **2011**, *44*, 3649–3655.

30 R. Israels, F. Leermakers, G. J. Fleer, E. B. Zhulina, *Macromolecules* **1994**, *27*, 3249–3261.

31 K. N. Witte, Y. Y. Won, *Macromolecules* **2006**, *39*, 7757–7768.

32 N. A. Kumar, C. Seidel, *Macromolecules* **2005**, *38*, 9341–9350.

33 Y. P. Ou, J. B. Sokoloff, M. J. Stevens, *Phys. Rev. E* **2012**, *85*, 011801.

34 F. Goujon, A. Ghoufi, P. Malfreyt, D. J. Tildesley, *Soft Matter* **2013**, *9*, 2966–2972.

35 S. Minko, M. Müller, D. Usov, A. Scholl, C. Froeck, M. Stamm, *Phys. Rev. Lett.* **2002**, *88*, 035502.

36 S. M. Hur, A. L. Frischknecht, D. L. Huber, G. H. Fredrickson, *Soft Matter* **2011**, *7*, 8776–8788.

37 S. M. Hur, A. L. Frischknecht, D. L. Huber, G. H. Fredrickson, *Soft Matter* **2013**, *9*, 5341–5354.

38 J. R. Roan, *Int. J. Mod. Phys. B* **2004**, *18*, 2469–2475.

39 J. R. Roan, *Phys. Rev. Lett.* **2006**, *96*, 248301.

40 Y. Q. Wang, G. Yang, P. Tang, F. Qiu, Y. L. Yang, L. Zhu, *J. Chem. Phys.* **2011**, *134*, 134903.

41 D. J. Li, X. Sheng, B. Zhao, *J. Am. Chem. Soc.* **2005**, *127*, 6248–6256.

42 B. Zhao, L. Zhu, *J. Am. Chem. Soc.* **2006**, *128*, 4574–4575.

43 L. Zhu, B. Zhao, *J. Phys. Chem. B* **2008**, *112*, 11529–11536.

44 X. M. Jiang, B. Zhao, G. J. Zhong, N. X. Jin, J. M. Horton, L. Zhu, R. S. Hafner, T. P. Lodge, *Macromolecules* **2010**, *43*, 8209–8217.

45 C. H. Bao, S. D. Tang, J. M. Horton, X. M. Jiang, P. Tang, F. Qiu, L. Zhu, B. Zhao, *Macromolecules* **2012**, *45*, 8027–8036.

46 Y. Y. Mai, L. Xiao, A. Eisenberg, *Macromolecules* **2013**, *46*, 3183–3189.

47 B. B. Wang, B. Li, B. Zhao, C. Y. Li, *J. Am. Chem. Soc.* **2008**, *130*, 11594–11595.

48 K. Sill, T. Emrick, *Chem. Mater.* **2004**, *16*, 1240–1243.

49 E. M. Sevick, *Macromolecules* **1996**, *29*, 6952–6958.

50 M. Manghi, M. Aubouy, C. Gay, C. Ligoure, *Eur. Phys. J. E* **2001**, *5*, 519–530.

51 D. I. Dimitrov, A. Milchev, K. Binder, D. W. Heermann, *Macromol. Theory Simul.* **2006**, *15*, 573–583.

52 A. G. Koutsioubas, N. Spiliopoulos, D. L. Anastassopoulos, A. A. Vradis, C. Toprakcioglu, *J. Chem. Phys.* **2009**, *131*, 044901.

53 S. A. Egorov, A. Milchev, L. Klushin, K. Binder, *Soft Matter* **2011**, *7*, 5669–5676.

54 K. Prochazka, *J. Phys. Chem.* **1995**, *99*, 14108–14116.

55 Z. Limpouchova, D. Viduna, K. Prochazka, *Macromolecules* **1997**, *30*, 8027–8035.

56 N. Ayres, *Polym. Chem.* **2010**, *1*, 769–777.

57 B. Zhao, L. Zhu, *Macromolecules* **2009**, *42*, 9369–9383.

58 T. Chen, I. Amin, R. Jordan, *Chem. Soc. Rev.* **2012**, *41*, 3280–3296.

59 O. Azzaroni, *J. Polym. Sci. Part A: Polym. Chem.* **2012**, *50*, 3225–3258.

60 K. Binder, A. Milchev, *J. Polym. Sci. Part B: Polym. Phys.* **2012**, *50*, 1515–1555.

61 M. E. Welch, C. K. Ober, *J. Polym. Sci. Part B: Polym. Phys.* **2013**, *51*, 1457–1472.

62 L. Ionov, N. Houbenov, A. Sidorenko, M. Stamm, S. Minko, *Adv. Funct. Mater.* **2006**, *16*, 1153–1160.

63 M. C. LeMieux, D. Julthongpiput, K. N. Bergman, P. D. Cuong, H. S. Ahn, Y. H. Lin, V. V. Tsukruk, *Langmuir* **2004**, *20*, 10046–10054.

64 I. Luzinov, S. Minko, V. V. Tsukruk, *Prog. Polym. Sci.* **2004**, *29*, 635–698.

65 S. Minko, M. Müller, M. Motornov, M. Nitschke, K. Grundke, M. Stamm, *J. Am. Chem. Soc.* **2003**, *125*, 3896–3900.

66 M. Motornov, R. Sheparovych, R. Lupitskyy, E. MacWilliams, S. Minko, *J. Colloid Interface Sci.* **2007**, *310*, 481–488.

67 Y. L. Xu, X. Q. Chen, X. Han, S. H. Xu, H. L. Liu, Y. Hu, *Langmuir* **2013**, *29*, 4988–4997.

68 E. S. Gil, S. M. Hudson, *Prog. Polym. Sci.* **2004**, *29*, 1173–1222.

69 X M. Jiang, B. B. Wang, C. Y. Li, B. Zhao, *J. Polym. Sci. Part A: Polym. Chem.* **2009**, *47*, 2853–2870.

70 J. F. Wang, M. Müller, *J. Phys. Chem. B* **2009**, *113*, 11384–11402.

71 S. Minko, S. Patil, V. Datsyuk, F. Simon, K. J. Eichhorn, M. Motornov, D. Usov, I. Tokarev, M. Stamm, *Langmuir* **2002**, *18*, 289–296.

72 L. Ionov, S. Minko, M. Stamm, J. F. Gohy, R. Jerome, A. Scholl, *J. Am. Chem. Soc.* **2003**, *125*, 8302–8306.

73 M. Y. Paik, Y. Y. Xu, A. Rastogi, M. Tanaka, Y. Yi, C. K. Ober, *Nano Lett.* **2010**, *10*, 3873–3879.

74 B. Helms, S. J. Guillaudeu, Y. Xie, M. McMurdo, C. J. Hawker, J. Frechet, *Angew. Chem. Int. Ed.* **2005**, *44*, 6384–6387.

75 B. Voit, *Angew. Chem. Int. Ed.* **2006**, *45*, 4238–4240.

76 P. E. Theodorakis, W. Paul, K. Binder, *Macromolecules* **2010**, *43*, 5137–5148.

77 P. E. Theodorakis, W. Paul, K. Binder, *Eur. Phys. J. E* **2011**, *34*, 52.

78 I. Erukhimovich, P. E. Theodorakis, W. Paul, K. Binder, *J. Chem. Phys.* **2011**, *134*, 054906.

79 P. G. de Gennes, Scaling Concepts in Polymer Physics, Cornell University Press: Ithaca, **1969**.

80 E. Zhulina, A. C. Balazs, *Macromolecules* **1996**, *29*, 2667–2673.

81 S. Alexander, *J. Phys.* **1976**, *38*, 977–981.

82 P. G. de Gennes, *J. Phys.* **1976**, *37*, 1445–1452.

83 P. G. de Gennes, *Macromolecules* **1980**, *13*, 1069–1075.

84 F. Schmid, *J. Phys.-Condes. Matter* **1998**, *10*, 8105–8138.

85 Y. L. Yang, F. Qiu, P. Tang, H. D. Zhang, *Sci. China B* **2006**, *49*, 21–43.

86 K. C. Daoulas, M. Müller, *J. Chem. Phys.* **2006**, *125*, 184904.

87 Y. X. Yu, J. Z. Wu, *J. Chem. Phys.* **2002**, *117*, 2368–2376.

88 D. Dukes, Y. Li, S. Lewis, B. Benicewicz, L. Schadler, S. K. Kumar, *Macromolecules* **2010**, *43*, 1564–1570.

89 M. Daoud, J. P. Cotton, *J. Phys.* **1982**, *43*, 531–538.

90 R. C. Van Lehn, A. Alexander-Katz, *J. Chem. Phys.* **2011**, *135*, 141106.

91 L. Wenning, M. Müller, K. Binder, *Europhys. Lett.* **2005**, *71*, 639–645.

92 K. Binder, *Rep. Prog. Phys.* **1997**, *60*, 487–559.

93 K. Binder, W. Paul, *Macromolecules* **2008**, *41*, 4537–4550.

94 M. Murat, G. S. Grest, *Macromolecules* **1989**, *22*, 4054–4059.

95 K. Kremer, G. S. Grest, *J. Chem. Phys.* **1990**, *92*, 5057–5086.

96 H. Merlitz, G. L. He, J. U. Sommer, C. X. Wu, *Macromolecules* **2009**, *42*, 445–451.

97 G. L. He, H. Merlitz, J. U. Sommer, C. X. Wu, *Macromolecules* **2009**, *42*, 7194–7202.

98 S. C. Glotzer, W. Paul, *Ann. Rev. Mater. Res.* **2002**, *32*, 401–436.

99 Y. H. Xue, H. Liu, Z. Y. Lu, X. Z. Liang, *J. Chem. Phys.* **2010**, *132*, 044903.

100 A. A. Rudov, P. G. Khalatur, I. I. Potemkin, *Macromolecules* **2012**, *45*, 4870–4875.

101 E. Moeendarbary, T. Y. Ng, M. Zangeneh, *Int. J. Appl. Mech.* **2009**, *1*, 737–763.

102 J. F. Marko, T. A. Witten, *Macromolecules* **1992**, *25*, 296–307.

103 H. Dong, *J. Phys. II France* **1993**, *3*, 999–1020.

104 K. G. Soga, M. J. Zuckermann, H. Guo, *Macromolecules* **1996**, *29*, 1998–2005.

105 Y. H. Yin, R. Jiang, B. H. Li, Q. H. Jin, D. T. Ding, A. C. Shi, *J. Chem. Phys.* **2008**, *129*, 154903.

106 H. M. Gao, H. Liu, Z. Y. Lu, Z. Y. Sun, L. J. An, *J. Chem. Phys.* **2013**, *138*, 224905.

107 H. Dong, J. F. Marko, T. A. Witten, *Macromolecules* **1994**, *27*, 6428–6442.

108 G. Brown, A. Chakrabarti, J. F. Marko, *Macromolecules* **1995**, *28*, 7817–7821.

109 P. G. Ferreira, L. Leibler, *J. Chem. Phys.* **1996**, *105*, 9362–9370.

110 E. B. Zhulina, C. Singh, A. C. Balazs, *Macromolecules* **1996**, *29*, 6338–6348.

111 E. B. Zhulina, C. Singh, A. C. Balazs, *Macromolecules* **1996**, *29*, 8254–8259.

112 Y. H. Yin, P. C. Sun, B. H. Li, T. H. Chen, Q. H. Jin, D. T. Ding, A. C. Shi, *Macromolecules* **2007**, *40*, 5161–5170.

113 R. Jiang, B. H. Li, Z. Wang, Y. H. Yin, A. C. Shi, *Macromolecules* **2012**, *45*, 4920–4931.

114 K. Gong, B. D. Marshall, W. G. Chapman, *J. Chem. Phys.* **2012**, *137*, 154904.

115 B. Zhao, W. J. Brittain, *J. Am. Chem. Soc.* **1999**, *121*, 3557–3558.

116 B. Zhao, W. J. Brittain, W. S. Zhou, S. Cheng, *Macromolecules* **2000**, *33*, 8821–8827.

117 L. J. Fetters, A. D. Kiss, D. S. Pearson, G. F. Quack, F. J. Vitus, *Macromolecules* **1993**, *26*, 647–654.

118 S. Santer, A. Kopyshev, J. Donges, J. Ruhe, X. G. Jiang, B. Zhao, M. Müller, *Langmuir* **2007**, *23*, 279–285.

119 Domain memory is a characteristic that quantifies to what extent domains form at the same position and with the same size/shape when the morphology of the brush is cyclically changed (e.g., through periodic exposure of the brush to two solvents of different quality). Domain memory also has its origin in the inhomogeneous distribution of grafting points, so it can be used to measure the correlations between fluctuations in the grafting-point positions and morphology in experiments. (a) S. Santer, A. Kopyshev, H. K. Yang, J. Ruhe, *Macromolecules* **2006**, *39*, 3056–3064; (b) S. Santer, A. Kopyshev, J. Donges, H. K. Yang, J. Ruhe, *Langmuir* **2006**, *22*, 4660–4667.

120 J. F. Wang, M. Müller, *Langmuir* **2010**, *26*, 1291–1303.

121 A. D. Price, S. M. Hur, G. H. Fredrickson, A. L. Frischknecht, D. L. Huber, *Macromolecules* **2012**, *45*, 510–524.

122 H. M. Xiong, J. X. Zheng, R. A. Van Horn, K. U. Jeong, R. P. Quirk, B. Lotz, E. L. Thomas, W. J. Brittain, S. Cheng, *Polymer* **2007**, *48*, 3732–3738.

123 W. H. Huang, C. X. Luo, J. L. Zhang, K. Yu, Y. C. Han, *Macromolecules* **2007**, *40*, 8022–8030.

124 R. C. Ball, J. F. Marko, S. T. Milner, T. A. Witten, *Macromolecules* **1991**, *24*, 693–703.

125 J. Pyun, K. Matyjaszewski, *Chem. Mater.* **2001**, *13*, 3436–3448.

126 C. R. Vestal, Z. J. Zhang, *J. Am. Chem. Soc.* **2002**, *124*, 14312–14313.

127 M. Chanana, S. Jahn, R. Georgieva, J. F. Lutz, H. Baumler, D. Y. Wang, *Chem. Mater.* **2009**, *21*, 1906–1914.

128 C. Boyer, M. R. Whittaker, M. Luzon, T. P. Davis, *Macromolecules* **2009**, *42*, 6917–6926.

129 C. Boyer, M. R. Whittaker, K. Chuah, J. Q. Liu, T. P. Davis, *Langmuir* **2010**, *26*, 2721–2730.

130 L. Chen, H. A. Klok, *Soft Matter* **2013**, *9*, 10678–10688.

131 E. R. Zubarev, J. Xu, A. Sayyad, J. D. Gibson, *J. Am. Chem. Soc.* **2006**, *128*, 15098–15099.

132 J. B. Song, L. Cheng, A. P. Liu, J. Yin, M. Kuang, H. W. Duan, *J. Am. Chem. Soc.* **2011**, *133*, 10760–10763.

133 J. He, Z. J. Wei, L. Wang, Z. Tomova, T. Babu, C. Y. Wang, X. J. Han, J. T. Fourkas, Z. H. Nie, *Angew. Chem. Int. Ed.* **2013**, *52*, 2463–2468.

134 Y. Guo, S. Harirchian-Saei, C. Izumi, M. G. Moffitt, *ACS Nano* **2011**, *5*, 3309–3318.

135 R. H. Zheng, G. J. Liu, X. H. Yan, *J. Am. Chem. Soc.* **2005**, *127*, 15358–15359.

136 K. Q. Chen, D. H. Liang, J. Tian, L. Q. Shi, H. Y. Zhao, *J. Phys. Chem. B* **2008**, *112*, 12612–12617.

137 A. M. Jackson, J. W. Myerson, F. Stellacci, *Nat. Mater.* **2004**, *3*, 330–336.

138 G. A. DeVries, M. Brunnbauer, Y. Hu, A. M. Jackson, B. Long, B. T. Neltner, O. Uzun, B. H. Wunsch, F. Stellacci, *Science* **2007**, *315*, 358–361.

139 C. Singh, P. K. Ghorai, M. A. Horsch, A. M. Jackson, R. G. Larson, F. Stellacci, S. C. Glotzer, *Phys. Rev. Lett.* **2007**, *99*, 226106.

140 I. C. Pons-Siepermann, S. C. Glotzer, *Soft Matter* **2012**, *8*, 6226–6231.

141 I. C. Pons-Siepermann, S. C. Glotzer, *ACS Nano* **2012**, *6*, 3919–3924.

142 V. N. Manoharan, M. T. Elsesser, D. J. Pine, *Science* **2003**, *301*, 483–487.

143 V. Khanna, E. W. Cochran, A. Hexemer, G. E. Stein, G. H. Fredrickson, E. J. Kramer, X. Li, J. Wang, S. F. Hahn, *Macromolecules* **2006**, *39*, 9346–9356.

144 B. Vorselaars, J. U. Kim, T. L. Chantawansri, G. H. Fredrickson, M. W. Matsen, *Soft Matter* **2011**, *7*, 5128–5137.

145 J. J. Thomson, *Philos. Mag.* **1904**, *7*, 237–265.

146 J. Q. Dong, J. Zhou, *Macromol. Theory Simul.* **2013**, *22*, 174–186.

147 G. M. Grason, R. D. Kamien, *Phys. Rev. E* **2005**, *71*, 051801.

148 C. I. Huang, L. F. Yang, *Macromolecules* **2010**, *43*, 9117–9125.

149 R. M. Hernandez, L. Richter, S. Semancik, S. Stranick, T. E. Mallouk, *Chem. Mater.* **2004**, *16*, 3431–3438.

150 C. D. Keating, M. J. Natan, *Adv. Mater.* **2003**, *15*, 451–454.

151 C. Singh, Y. Hu, B. P. Khanal, E. R. Zubarev, F. Stellacci, S. C. Glotzer, *Nanoscale* **2011**, *3*, 3244–3250.

152 W. L. Miller, B. Bozorgui, K. Klymko, A. Cacciuto, *J. Chem. Phys.* **2011**, *135*, 244902.

153 S. A. Egorov, *Soft Matter* **2012**, *8*, 3971–3979.

154 C. Tung, A. Cacciuto, *J. Chem. Phys.* **2013**, *139*, 194902.

155 X. Ma, Y. Z. Yang, L. Zhu, B. Zhao, P. Tang, F. Qiu, *J. Chem. Phys.* **2013**, *139*, 214902.

156 X. Ma, C. Y. Chen, P. Tang, F. Qiu, *Acta Chim. Sin.* **2014**, *72*, 208–214.

157 C. Singh, G. T. Pickett, A. C. Balazs, *Macromolecules* **1996**, *29*, 7559–7570.

158 C. Singh, G. T. Pickett, E. Zhulina, A. C. Balazs, *J. Phys. Chem. B* **1997**, *101*, 10614–10624.

159 K. Kremer, M. O. Robbins, G. S. Grest, *Phys. Rev. Lett.* **1986**, *57*, 2694–2697.

160 Y. Monovoukas, A. P. Gast, *J. Colloid Interface Sci.* **1989**, *128*, 533–548.

161 Z. L. Zhang, M. A. Horsch, M. H. Lamm, S. C. Glotzer, *Nano Lett.* **2003**, *3*, 1341–1346.

162 A. Santos, J. A. Millan, S. C. Glotzer, *Nanoscale* **2012**, *4*, 2640–2650.

163 K. Kanie, M. Matsubara, X. B. Zeng, F. Liu, G. Ungar, H. Nakamura, A. Muramatsu, *J. Am. Chem. Soc.* **2012**, *134*, 808–811.

164 K. Ohno, T. Morinaga, S. Takeno, Y. Tsujii, T. Fukuda, *Macromolecules* **2006**, *39*, 1245–1249.

165 K. Ohno, T. Morinaga, S. Takeno, Y. Tsujii, T. Fukuda, *Macromolecules* **2007**, *40*, 9143–9150.

166 D. Nykypanchuk, M. M. Maye, D. van der Lelie, O. Gang, *Nature* **2008**, *451*, 549–552.

167 S. Y. Park, A. Lytton-Jean, B. Lee, S. Weigand, G. C. Schatz, C. A. Mirkin, *Nature* **2008**, *451*, 553–556.

168 T. B. Martin, A. Seifpour, A. Jayaraman, *Soft Matter* **2011**, *7*, 5952–5964.

169 C. E. Estridge, A. Jayaraman, *J. Chem. Phys.* **2014**, *140*, 144905.

170 V. V. Ginzburg, *Macromolecules* **2013**, *46*, 9798–9805.

171 M. Nuopponen, H. Tenhu, *Langmuir* **2007**, *23*, 5352–5357.

172 L. Cheng, A. P. Liu, S. Peng, H. W. Duan, *ACS Nano* **2010**, *4*, 6098–6104.